

1 **Re-appraising the role of T-cell derived interferon gamma in restriction of *Mycobacterium*
2 *tuberculosis* in the murine lung**

3
4 **T-cell derived IFN γ is required to restrict pulmonary *Mtb***

5
6 Karolina Maciag^{1,2}, Courtney Plumlee¹, Sara Cohen¹, Benjamin Gern¹, Kevin Urdahl^{1,3*}

7 ¹Seattle Children's Research Institute; ²Division of Allergy and Infectious Diseases, University of
8 Washington; ³Department of Immunology, University of Washington

9
10

11 **ABSTRACT**

12 T cells producing interferon gamma (IFNy) have long been considered a stalwart for immune protection
13 against *Mycobacterium tuberculosis* (*Mtb*), but their relative importance to pulmonary immunity has been
14 challenged by murine studies which achieved protection by adoptively transferred *Mtb*-specific IFNy^{-/-} T
15 cells. Using IFNy^{-/-} T cell chimeric mice and adoptive transfer of IFNy^{-/-} T cells into TCR $\beta^{-/-}\delta^{-/-}$ mice, we
16 demonstrate that control of lung *Mtb* burden is in fact dependent on T cell-derived IFNy, and furthermore,
17 mice selectively deficient in T cell-derived IFNy develop exacerbated disease compared to T cell-
18 deficient controls despite equivalent lung bacterial burdens. Deficiency in T cell-derived IFNy skews
19 infected and bystander monocyte-derived macrophages (MDMs) to an alternative M2 phenotype, and
20 promotes neutrophil and eosinophil influx. Our studies support an important role for T cell-derived IFNy in
21 pulmonary immunity against TB.

22

23 **INTRODUCTION**

24 Studies in mice and in human cells have repeatedly demonstrated that immunity to *Mtb* requires both T
25 cells and IFNy. Genetic deficiencies in CD4+ T cells are associated with increased susceptibility to *Mtb* in
26 mice(1) and humans(2), an outcome mirrored during acquired CD4+ deficiency in advanced HIV(3). Global
27 knockout studies have likewise confirmed the importance of IFNy in *Mtb* restriction in mice(4, 5), and
28 deficits in IFNy signaling are associated with human susceptibility to mycobacterial infections – most often
29 with environmentally ubiquitous non-tuberculous mycobacteria, but also TB (6). Nevertheless, the relative
30 contribution of T cell-derived IFNg to protective immunity remains unclear. Currently, vaccine candidates
31 are routinely assessed on their ability to elicit T cell memory responses – particularly, the ability of
32 peripheral blood T cells to produce interferon gamma (IFNy) - but this parameter does not consistently
33 correlate with protective immunity to *Mtb*(7–14). Additionally, IFNy-producing T cells can contribute to
34 amelioration(15) or exacerbation(16) of lung pathology in the context of *Mtb* infection. Studies on the
35 importance of polyfunctional CD4+ T cells, as well as in vivo(15–18) and in vitro(19) studies suggestive
36 of IFNy-independent CD4+ T cell functions, have cast doubt on the primacy of T cell-derived IFNy. IFNy
37 is produced by other cell types in addition to T cells during *Mtb* infection(20), and the relationship
38 between IFNy and its source and target cells remains incompletely understood. Understanding the
39 relative role of T cell-derived IFNy will inform a rational approach to inducing vaccine-mediated protection
40 against tuberculosis(11, 14).

41

42 Prior T cell adoptive transfer studies in mice on the C57BL/6 genetic background have challenged the
43 relative importance of T cell-derived IFNy in immunity to *Mtb*. In *Mtb*-infected RAG2^{-/-} host mice, adoptive
44 transfer of CD4+ T cells from previously *Mtb*-infected, antibiotic-treated donor mice reduced *Mtb* lung
45 burden and conferred a survival advantage relative to no-transfer control mice whether or not donor T
46 cells expressed IFNy(10). In another study, adoptive transfer of naïve CD4+ T cells from uninfected

47 donor mice into *Mtb*-infected RAG1^{-/-} mice reduced *Mtb* burden in the lung in a manner only partially
48 dependent on donor T cell IFN γ (16). Finally, in WT mice, adoptive transfer of *in vitro* Th1-polarized CD4+
49 TCR-transgenic T cells specific for the immunodominant *Mtb* antigen ESAT6 reduced *Mtb* burden in a
50 manner partially – or, at high doses of transferred cells, completely – independently of donor T cell-
51 derived IFN γ (18). Together, these reports suggest that CD4+ T cell-derived IFN γ plays a minimal(18) or
52 partial(15, 16) role in protective immunity against *Mtb* within the lung.

53

54 While these studies highlight potential roles of T cell immunity beyond IFN γ , the adoptive transfer
55 techniques employed carry limitations that may lead to underestimation of the relative importance of T
56 cell-derived IFN γ . For example, transfer of a fixed quantity of T cells into lymphopenic mice leads to a
57 limited T cell repertoire (21), potentially skewing the resulting immune response. In this scenario,
58 adoptively transferred T cells also undergo rapid proliferation, differentiation, and activation(21, 22),
59 which would alter their response to subsequent infection and can lead to systemic autoimmunity(23). In
60 addition, RAG-deficient host mice lack not only T cell function but also lack mature B cells and normal
61 lymphoid structure(24). In TCR-transgenic adoptive transfer studies, a very large number of monoclonal
62 *Mtb*-specific T cells may amplify the relative contribution of IFN γ -independent mechanisms of protection
63 that may play a minor role in a more physiologic *Mtb*-specific cell response. Here, we use a T cell bone
64 marrow chimera model to address some of the shortcomings of prior adoptive transfer studies and to re-
65 assess the hypothesis that T cell-derived IFN γ plays only a minor role in T cell-dependent immunity to
66 *Mtb* in the lung. In contrast to methods used in prior studies, we use the more specific T cell-deficient
67 TCR β ^{-/-} δ ^{-/-} host strain, and the T cell chimera model allows physiologically relevant T cell development,
68 including generation of a diverse TCR repertoire, thymic selection, and homeostatic regulation, to occur
69 in the host mouse (25). Our findings indicate that T cell-derived IFN γ is indeed essential for pulmonary
70 immune protection against *Mtb*, providing a reappraisal of the relative importance of this aspect of T cell
71 mediated immunity.

72

73 MATERIALS AND METHODS

74 *Mice*

75 TCR β ^{-/-} δ ^{-/-} (strain #002122), IFN γ ^{-/-} (strain #002287), and C57BL/6J (wildtype, strain #000664) mice were
76 obtained from Jackson Laboratories (Bar Harbor, ME). Mice were matched by age (when possible) and
77 sex. Mice across different experimental groups were co-housed in the same cage in order to minimize
78 confounding differences in environment and microbiota. Mice were sacrificed using cervical dislocation.
79 All animals were housed and maintained in specific-pathogen-free conditions at Seattle Children's
80 Research Institute (SCRI). All animal studies were performed with approval of the SCRI Animal Care and
81 Use Committee.

82

83 *Bone marrow chimeras*

84 Recipient TCR $\beta^{-/-}$ mice were sublethally irradiated with 600 rads. Bone marrow was prepared from
85 femurs and tibias of TCR $\beta^{-/-}$, WT, and IFN $\gamma^{-/-}$ donor mice, and depleted of mature T cells using a CD3 ε
86 depletion kit (Miltenyi Biotec, #130-094-973). 1-2x10 6 bone marrow cells were then injected retro-orbitally
87 to each host mouse under isoflurane anesthesia. Mice received enrofloxacin in drinking water for four
88 weeks after irradiation to prevent neutropenic sepsis. Chimeric mice were rested for 8-10 weeks prior to
89 subsequent manipulation to allow for T cell development.

90

91 *Adoptive transfer*

92 Adoptive transfer of total CD4 T cells into immunocompromised host mice was performed 7 days after
93 aerosol *Mtb* infection of host TCR $\beta^{-/-}$ or RAG1 $^{-/-}$ mice as follows. CD4+ T cells were isolated from
94 spleens and lymph nodes of donor C57BL/6 and IFN $\gamma^{-/-}$ mice using the MagniSort CD4+ T cell
95 enrichment kit (ThermoFisher, #8804-6821-74). Flow cytometry confirmed that >85% of isolated live
96 CD4+ T cells were naïve (CD44loCD62Lhi). 3x10 6 CD4+ T cells were injected retro-orbitally to each host
97 mouse under isoflurane anesthesia.

98

99 *Mtb aerosol infections*

100 T cell chimeric mice were infected with 25-100 CFU aerosolized *Mtb* H37Rv transformed with a reported
101 plasmid bearing the mCherry fluorescent marker constitutively expressed under the pMSP12 promoter
102 sequence(26). Adoptive transfer mice were infected with 25-100 CFU aerosolized *Mtb* H37Rv. Aerosol
103 infections were performed in a Glas-Col chamber. Two additional mice in each infection were sacrificed
104 directly after infection to confirm the infectious dose of *Mtb* CFU per mouse.

105

106 *CFU plating*

107 Mouse lung lobes and spleens were homogenized in M tubes (Miltenyi Biotec) containing 1mL
108 PBS+0.05% Tween-80 (PBS-T) using a GentleMACS tissue dissociator (Miltenyi Biotec). Organ
109 homogenates were then diluted in PBS-T and aliquots were plated onto 7H10 agar media to quantify *Mtb*
110 burden. Plates were incubated at for 37°C for at least 21 days prior to CFU counting.

111

112 *Flow cytometry*

113 CD45.2 antibody (0.2 mg, PE) was injected into mice retro-orbitally 5-10 minutes prior to sacrifice to label
114 intravascular cells. Lung lobes were excised and dissociated in C tubes (Miltenyi Biotec) in HEPES buffer
115 containing Liberase Blendzyme 3 (70 mg/ml; Roche) and DNaseI (30 mg/ml; Sigma-Aldrich) using a
116 GentleMACS dissociator (Miltenyi Biotec). Lung homogenates were incubated for 30 minutes at 37°C
117 and further processed with the GentleMACS dissociator. Cell suspensions were filtered through a 100
118 μ m cell strainer, treated with RBC lysis buffer (Thermo), and resuspended in FACS buffer (PBS

119 containing 2.5% FBS and 0.1% NaN3). Single cell suspensions were washed in PBS and then incubated
120 with 50 μ l Zombie Aqua viability dye (BioLegend) for 10 minutes at room temperature in the dark. Cell
121 markers were stained and viability dye was quenched by the addition of 100 μ l of a cocktail of
122 fluorophore-conjugated antibodies diluted in 50% FACS buffer/50% 24G2 Fc block (Bio X Cell, 2.4G2),
123 and incubated for 20 minutes at 4°C. Cells were washed once with FACS buffer and fixed with 1%
124 paraformaldehyde for 30 minutes prior to analysis on an LSRII flow cytometer (BD Biosciences).
125

126 *Cell sorting*

127 Lungs were processed as described for flow cytometry above, but NaN3 was omitted from FACS buffer.
128 Cells were sorted on a FACSAria cell sorter (BD Biosciences) under BSL3 conditions.
129

130 *RNA-seq*

131 Single cell suspensions from lung were analyzed and sorted by fluorescence-activated flow cytometry
132 (FACS) into *Mtb*-infected (mCherry+) and bystander (mCherry-) MDM (dead- SiglecF- Ly6G- CD11b+
133 CD64+) populations. RNA was isolated using Trizol, and quantified using bulk RNA-seq (Psomagen)
134 after construction of Illumina sequencing libraries using the SMARTer Stranded Total RNA-Seq Kit v3 -
135 Pico Input Mammalian (Takara). Noise from low-expression transcripts was filtered, and analysis of
136 differentially expressed genes (DEGs) across groups was done using the edgeR module in R(27).
137

138 *Protein quantification*

139 Lung lobes were homogenized in M tubes (Miltenyi Biotec) containing 1ml of ProcartaPlex Cell Lysis
140 Buffer (Invitrogen EPX-99999-000) with Halt Protease Inhibitor (Invitrogen 78440) and DNase (30 mg/ml;
141 Sigma-Aldrich) using a GentleMACS tissue dissociator (Miltenyi Biotec). Homogenates were centrifuged
142 to pellet debris, and supernatants were filtered twice through a 0.22 μ m pore size Costar SpinX column
143 (Corning) to exclude mycobacteria, frozen at -80°C, and assayed after a single freeze-thaw cycle. Total
144 protein was measured by bicinchoninic acid (BCA) assay (ThermoFisher), and these values were used to
145 normalize individual analyte levels in each sample. IL-4, IL-5, and IL-13 levels in lung homogenates were
146 measured using Cytokine Bead Array Flex Sets (BD); bead fluorescence was measured on an LSRII flow
147 cytometer (BD Biosciences) and analyzed by four-parameter log-logistic curve-fitting to the standard
148 curve. IFNy levels were quantified using a magnetic Luminex assay (ThermoFisher Scientific) and
149 analyzed using BioPlex Manager software (Bio-Rad).
150

151 *Histopathologic analysis and confocal imaging*

152 Right inferior lung lobes were dissected and fixed in 20ml of 1:3 dilution of BD Cytofix Buffer (~1%
153 formaldehyde) for 24hr at 4°C to ensure killing of *M. tuberculosis*, equilibrated in 30% sucrose solution
154 for another 24hr at 4°C, then rapidly frozen in OCT in an ethanol-dry ice slurry and stored at -80°C. For

155 histopathologic analysis, tissue was embedded in paraffin, 4mm tissue sections were prepared with a
156 cryostat and mounted on glass slides, stained with hematoxylin-eosin by the UW Comparative Pathology
157 Core Facility, then assessed by a trained veterinary pathologist blinded to group assignments. For
158 confocal imaging, 20mm tissue sections were prepared with a cryostat and mounted on glass slides.
159 Sections were stained with fluorophore-conjugated antibodies and Nucspot 750/780 nuclear stain
160 (Biotium) overnight at room temperature and coverslipped with Fluoromount G mounting media
161 (Southern Biotec). Images were acquired on a Leica Stellaris 8 confocal microscope, compensated for
162 fluorophore spillover using LAS X (Leica), and rendered in Imaris (Bitplane), where ARG1 signal was
163 smoothed using a Gaussian filter with a width of 0.316 μ m. Identical settings were applied across
164 experimental groups.

165

166 *Statistical analysis*

167 Statistical significance was determined using the multcomp and rstatix packages in R, using methods
168 indicated in the figure legends. Principal component analysis was done using the stats package in R.
169

170 RESULTS

171 ***T cell-derived IFNy is required to reduce lung Mtb burden, and protect from disease.***

172 To investigate the role of T cell-derived IFNy in TB immunity, we generated T cell chimeric mice (**Fig. 1A**)
173 in which T cells, but not other cell types, were genetically deficient in their capacity to express IFNy. To
174 establish this system, TCR $\beta^{-/-}$ host mice were partially myeloablated by sublethal irradiation and
175 reconstituted with bone marrow of IFNy $^{-/-}$ donor mice, or as controls, bone marrow of TCR $\beta^{-/-}$ or WT
176 mice. In these chimeras, all T cells are derived from the donor bone marrow (e.g., IFNy $^{-/-}$ for the
177 experimental group), whereas >95% of other hematopoietic lineage cells remain wildtype due to the
178 sublethal dose of radiation(25). After immune reconstitution, T cell chimeric mice were infected with
179 aerosolized *Mtb* H37Rv, then assessed for bacterial burden in lungs and spleens at 25 days post
180 infection (dpi). In contrast to prior T cell transfer studies suggesting that T cell-derived IFNy may be
181 partially or wholly dispensable for protective T cell responses against murine pulmonary *Mtb*(16, 18), we
182 found that control of bacterial burden in lungs and spleens of T cell chimeric mice at 25dpi was indeed
183 dependent on T cell-derived IFNy (**Fig. 1B-C**). Furthermore, IFNy $^{-/-}$ T cell chimeric mice exhibited clinical
184 deterioration (decreased activity, hunched posture) and lost weight beyond 25dpi, while TCR $\beta^{-/-}$
185 chimeric controls did not (**Fig. 1D**), despite equivalent lung bacterial burdens, suggesting that T cell
186 activity during *Mtb* infection promotes disease unless countered by T cell-derived IFNy.

187

188 In contrast to our results in the T cell chimera model, prior studies have shown that adoptive transfer of
189 IFNy $^{-/-}$ T cells into T cell-deficient (RAG1 $^{-/-}$) host mice decreases lung and spleen *Mtb* CFU relative to no
190 transfer, though the protective effect was smaller than that observed after adoptive transfer of WT T

191 cells(16). We used a similar adoptive transfer strategy (**Fig. 2A**) to reconcile those findings with our
192 results. Instead of RAG-deficient host mice as in Sakai et al., however, we used TCR $\beta^{-/-}$ host mice (as
193 we had used in the T cell chimera experiments, **Fig. 1A**). TCR $\beta^{-/-}$ host mice were infected with
194 aerosolized *Mtb* and CD4+ T cells (3x10⁶/mouse) isolated from WT or IFN $\gamma^{-/-}$ donor mice were
195 administered intravenously at 7dpi. In order to investigate whether IFN $\gamma^{-/-}$ T cells mediate pathologic
196 effects, and whether WT T cells can counteract those effects in this model, an additional group of mice
197 received a 50% / 50% mix of WT and IFN $\gamma^{-/-}$ T cells. Similarly to our observations in T cell chimeric
198 animals, WT T cells significantly decreased *Mtb* burden in both the lungs and spleens of TCR $\beta^{-/-}$ host
199 mice at 36dpi, while IFN $\gamma^{-/-}$ T cells did not (**Fig. 2B**), again supporting a requirement for T cell-derived
200 IFN γ for control of bacterial burden in murine *Mtb* infection. Furthermore, mice receiving adoptively
201 transferred IFN $\gamma^{-/-}$ CD4+ T cells exhibited significantly more weight loss over the course of infection than
202 either no-transfer controls or WT CD4+ T cell transfer mice (**Fig. 2C**), despite having equivalent
203 mycobacterial burdens as no-transfer controls. This is again consistent with a pathologic effect mediated
204 by T cells that are unable to produce IFN γ , as observed in T cell chimeric mice. Interestingly, co-
205 administration of WT and IFN $\gamma^{-/-}$ donor CD4+ T cells restored the ability of recipient mice to control
206 mycobacterial burden in lungs and spleens (**Fig. 2B**, “mix”), and decreased the rate of weight loss after
207 infection compared to mice receiving IFN $\gamma^{-/-}$ T cells alone. This suggests that IFN $\gamma^{-/-}$ deficient T cells are
208 not inherently pathogenic, and can be complemented *in trans* by the presence of other T cells that can
209 produce IFN γ – but not by other IFN γ -producing cell types (such as NK or NKT cells) during *Mtb*
210 infection.

211
212 In a parallel experiment, we also tested whether the difference between our results and those reported
213 by Sakai et al. could be explained by differences in the host mice used, as ours were specifically
214 deficient in T cells (TCR $\beta^{-/-}$), whereas Sakai et al. used mice deficient in both B and T cells (RAG1 $^{-/-}$)
215 (**Fig. S1A**). While Sakai et al. reported 60-fold and 5-fold decreases in lung and spleen *Mtb* burden in
216 RAG1 $^{-/-}$ mice that had received IFN $\gamma^{-/-}$ T cells compared to no-transfer control mice at 42dpi(16), we
217 observed similar lung and spleen mycobacterial burdens in these groups (**Fig. S1B**). However, we had to
218 assess mycobacterial burden in RAG1 $^{-/-}$ host mice at the earlier 34dpi timepoint since in our laboratory,
219 *Mtb*-infected RAG1 $^{-/-}$ host mice started to lose weight after 23 days of infection regardless of transferred
220 T cell genotype (**Fig. S1C**) and, in a separate experiment, many in fact required euthanasia prior to
221 42dpi. In addition, within-group variance among lung *Mtb* CFU in RAG1 $^{-/-}$ host mice in our hands was
222 high, which limited our ability to observe statistically significant intra-group effects in lung *Mtb* burden
223 (**Fig. S1B, left**) and thus may have also contributed to discordance between our findings and those of
224 Sakai et al. Although our results do not fully explain the discrepancy between our findings and those
225 previously published, they suggest that using RAG1 $^{-/-}$ recipients that lack both T cells and B cells and that
226 have aberrant lymph nodes may lead to confounding factors that increase variability in some settings.

227 Taken together, our data using both T cell chimeric mice and adoptive transfer into T cell-deficient mice
228 suggest that T cell derived IFNy is required for pulmonary immunity against *Mtb*, and that a T cell-specific
229 incapability to produce IFNy can in fact promote detrimental pathologic effects.

230

231 ***TB lesions in IFNy^{-/-} T cell chimeric mice exhibit increased neutrophilic and eosinophilic***
232 ***infiltration.***

233 To investigate the immune landscape associated in mice with T cell intrinsic IFNy deficiency, we
234 analyzed the cellular composition of lung tissue of T cell chimeric mice at 25dpi using flow cytometry
235 (**Fig. 3A**, gating as in **Fig. S2A**). Strikingly, the number of both neutrophils and eosinophils in IFNy^{-/-} T
236 cell chimeric mice was approximately ~1 log higher than in either TCR $\beta^{-/-}\delta^{-/-}$ (lacking T cells) or WT T cell
237 chimeras (**Fig. 3A**), though T cell-dependent recruitment of monocyte-derived macrophages (MDMs) was
238 preserved in both IFNy^{-/-} and WT T cell chimeras. Consistent with these findings, confocal microscopy
239 revealed robust neutrophil and eosinophil infiltration into pulmonary TB lesions in IFNy^{-/-} chimeric mice
240 (**Fig. 3B**).

241

242 We next asked whether histopathologic tissue analysis might help give insight into how increased
243 neutrophil and eosinophil responses (**Fig. 3A-B**) may be linked with clinical decline in IFNy^{-/-} T cell
244 chimeric mice relative to TCR $\beta^{-/-}\delta^{-/-}$ and WT T cell chimeras (**Fig. 1D**). Hematoxylin-eosin stained lung
245 sections were scored in a blinded fashion across eleven standardized histopathologic features (**Fig.**
246 **S3A**) confirming that *Mtb* lesions in IFNy^{-/-} T cell chimeric mouse lungs were marked by abundant
247 neutrophil and eosinophil infiltration (**Fig. S3B**, 800x). Absence of T cells correlated with fewer and more
248 poorly organized TB lesions in TCR $\beta^{-/-}\delta^{-/-}$ T cell chimeric mice, while both IFNy^{-/-} and WT T cell chimeric
249 mice were able to form dense, organized TB lesions (**Fig. S3B**, 25x). While the differences in
250 histopathology across groups were individually subtle, combined assessment using principal component
251 analysis of the blinded histopathology feature scores clustered samples within each genotype together,
252 indicating similar pathology; this was driven mainly by lesion neutrophils and eosinophils in IFNy^{-/-} T cell
253 chimeric mice, and decreased extent and severity of lung involvement, as well as absence of lymphoid
254 aggregates, in TCR $\beta^{-/-}\delta^{-/-}$ chimeric mice (**Fig. 3C**). In summary, T cells were able to promote organized
255 TB lesions in lung tissue of T cell chimeric mice during *Mtb* infection regardless of their ability to produce
256 IFNy, but T cell-derived IFNy was required to restrict neutrophil and eosinophil infiltration of these
257 lesions.

258

259 ***IFNy^{-/-} T cell chimeric mice exhibit a Th2 cytokine milieu and alternative activation of MDMs.***

260 To further investigate the possible immune effector mechanisms associated with the maladaptive
261 response to *Mtb* infection in IFNy^{-/-} T cell chimeric mice, we assessed gene expression in lung MDMs, the
262 primary infected cell type in pulmonary TB. In FACS-sorted *Mtb*-mCherry infected and bystander MDMs

263 at 25dpi, we noted prominent suppression of multiple hallmark M1 genes commonly associated with
264 antimycobacterial responses, including *Nos2*, *IL12a*, and *IL12b*, and concurrent upregulation of a subset
265 of hallmark alternative activation (M2) genes, including *Arg1*, *Chil3* (*Ym1*), *Mrc1* (*CD206*), *Fn1*, *Retnla*
266 (*Fizz1*), and *Ccl22* (**Fig. 4A**). Cytokine quantification in whole-lung lysates correlated the observed M2-
267 related gene expression in IFNy^{-/-} T cell chimera MDMs (**Fig. 4A**) with the presence of the canonical Th2
268 cytokines IL-4, IL-5, and IL-13, along with nearly complete absence of IFNy (**Fig. 4B**). Confocal
269 microscopy confirmed that, consistent with transcriptional data, expression of NOS2 was absent in lung
270 MDMs of IFNy^{-/-} T cell chimeric mice at 25dpi, while the M2 marker ARG1 was expressed on a much
271 greater proportion of MDMs (**Fig. 4C**). We asked whether the type 1 interferon response, which has been
272 associated with an ineffective and pathogenic response to *Mtb* infection(28–31) including neutrophil-
273 associated pathology(32), may be responsible for the shutdown of type 2 interferon responses in IFNy^{-/-}
274 T cell chimeras. However, transcription of both type 1 and type 2 interferon responses was suppressed in
275 IFNy^{-/-} T cell chimera mouse lung MDMs, suggesting that type 1 interferons do not play a major role in
276 suppressing type 2 interferon-induced responses in these mice (**Fig. S4**).
277

278 **DISCUSSION**

279 Despite prior reports that T cell-derived IFNy plays a minimal role in *Mtb* restriction in the C57BL/6
280 mouse model, our studies confirm it is indeed essential to control lung *Mtb* burden and disease in this
281 setting. Furthermore, our results indicate a detrimental role for T cell signals unopposed by concomitant
282 T cell-derived IFNy in pulmonary *Mtb* infection. Unopposed IFNy-independent T cell signaling correlates
283 with clinical decline and recruitment of neutrophils and eosinophils to *Mtb* lung lesions. These effects did
284 not involve a type 1 interferon response, but correlated with a Th2 cytokine signature and skewing of
285 MDMs to an M2 phenotype. Pathology was worse in IFNy^{-/-} compared to TCR $\beta^{-/-}\delta^{-/-}$ T cell chimeric mice
286 despite no statistical difference in lung *Mtb* CFU burden, suggesting that T cell-derived IFNy regulates
287 tolerance of the host to manifestations of disease from *Mtb* infection, such as tissue damage and weight
288 loss. An effective vaccine strategy against TB disease will likely require both IFNy-dependent and
289 independent T cell effects, and that – as is frequently the case for immune responses *in vivo* – a balance
290 between these two arms of the T cell response is required for effective protection while minimizing
291 immunopathology.
292

293 Pulmonary lesions in TB disease-susceptible IFNy^{-/-} T cell chimeric mice were marked by neutrophil and
294 eosinophil infiltration. Whether the recruitment of these cell types is a major driver of lung pathology and
295 clinical deterioration remains to be determined. While neutrophils may play a host-protective role in
296 mycobacterial clearance early in infection through phagocytosis and ROS production, adverse outcomes
297 in *Mtb* infection are usually associated with a dysregulated neutrophil response that plays a major role in
298 driving detrimental pathology(33). Prior studies have also shown that IFNyR^{-/-} neutrophils accumulate in

299 the lungs of *Mtb*-infected WT/IFNyR^{-/-} mixed bone marrow chimeric mice, and that these mice exhibit
300 accelerated weight loss(15), consistent with a direct role for IFNy in suppressing harmful neutrophil
301 accumulation in the lung during *Mtb* infection. Our results build on this model by suggesting that T cells
302 may provide an essential source of IFNy that inhibits the pathogenic effects of neutrophils. Whether the
303 abundant eosinophils we observed in pulmonary TB lesions of IFNy^{-/-} T cell chimeric mice also drive
304 detrimental pathology, or a potentially mediate a host-beneficial response to severe disease, deserves
305 further study. Prior work using two independent genetic models of global eosinophil deficiency
306 demonstrated a role for these cells in restriction of mycobacterial burden(34). However, the contribution
307 of eosinophils to the host-pathogen balance may be context-specific.

308

309 Lung lysates of *Mtb*-infected IFNy^{-/-} T cell chimeric mice were marked by a significant Th2 cytokine
310 profile, with abundant IL-4, IL-5, and IL-13. In prior murine studies, depletion of IL- 4 led to improved
311 control of *Mtb* burden in BALB/c mice (35). In C57BL/6 mice, known to have a strong Th1-skewed
312 response to *Mtb* infection, pulmonary *Mtb* burden was not affected by global deficiency in IL-4 or IL-
313 (36). However, over-expression of IL13 in C57BL/6 mice led to formation of necrotizing
314 granulomas(37) in an IL-4Ra-dependent manner(38). Further, alternatively activated M2 macrophages
315 expressing ARG1, associated with the presence of Th2 cytokines, were abundant in this model(37).
316 Accordingly, we observed suppression of the Th1-driven NOS2 and induction of the Th2-driven M2
317 marker ARG1 in macrophages in *Mtb* lesions of IFNy^{-/-} T cell chimeric mice. Consistent with these
318 findings, Th2 responses have been shown to be responsible for more severe pulmonary inflammation
319 and TB disease in mice exposed to *Schistosoma mansoni* parasites or antigen than in untreated mice
320 across a range of murine genotypes (39). Together, this evidence again suggests a context-specific
321 effect that may depend on factors including genetic background, helminth coinfection, and environment.

322

323 There is also mounting evidence from human clinical and experimental studies supporting a detrimental
324 role for Th2 cytokine signaling in TB pathology(40). A study of 1971 HIV-negative patients with sputum
325 culture-positive pulmonary TB in Ghana revealed that a variant of IL4-R α associated with increased
326 signal transduction was associated with increased cavity size(38). In addition, a significantly higher
327 IL-4/IFNy ratio was observed in stimulated lung lymphocytes from bronchoalveolar lavage (BAL) in
328 patients with miliary(41) or cavitary(42) rather than pleural(41) or non-cavitary(42) TB. The same pattern
329 was seen among peripheral blood lymphocytes(43), though the proportion of circulating IL-4-expressing
330 T cells was much smaller than in BAL when measured concurrently in the same patients(41), implying an
331 important role for tissue-specific responses. Indeed, in-situ hybridization using resected lung tissue from
332 patients with severe pulmonary TB demonstrated IFNy and IL-4 mRNA-producing cells within the same
333 granulomas, as well as co-existence of these mixed granulomas alongside granulomas expressing only
334 IFNy within the same patient(44); each lesion may therefore represent a unique cytokine micro-

335 environment. Thus, while Th2-associated comorbidities such as helminth infection or allergy/atopy have
336 not consistently correlated with severity of TB disease(45–47), studies have repeatedly demonstrated an
337 association between the ratio of Th2 vs Th1 cells and severity of *Mtb* infection outcomes. It has been
338 suggested that a vaccine that would protect against *Mtb* in areas where both TB and helminthic
339 infections are endemic should both support the Th1 response and block the Th2 response(40, 48). Our
340 findings correlating Th2 cytokines and M2 macrophage responses with severe TB disease support this
341 framework.

342

343 While T cell-derived IFNy is most often thought of in terms of its effect on macrophages, it is not known
344 which cellular target is primarily responsible for the differences in *Mtb* infection outcome between WT
345 and IFNy^{-/-} T cell chimeric mice. T cell-derived IFNy can be sensed by T cells themselves, and plays a
346 role in subsequent Th1 polarization(49). Furthermore, effects of IFNy on *Mtb* immunity have been
347 correlated with induction of gene expression in epithelial cells(50), and by shaping T cell compartments
348 by inducing apoptosis of activated CD4+ T cells(51). Future studies to characterize cell compartments,
349 apoptosis, and activation status in lungs of *Mtb*-infected IFNy^{-/-} T cell chimeric mice will help address this
350 question.

351

352 In a prior study, depletion of CD4+ T cells led to worsening *Mtb* infection outcomes in mice despite
353 relatively preserved levels of total IFNy in the lung(20). Notably, in our studies, production of lung IFNy
354 and expression of NOS2 by lung MDMs was even lower in IFNy^{-/-} T cell chimeric mice than in T cell
355 chimeras that lacked T cells completely. This suggests that there is IFNy production by cell types other
356 than T cells, such as NK or monocytic cells, which may expand in a compensatory manner when T cells
357 are absent – but these cells may be suppressed or unable to meaningfully increase IFNy production
358 when T cells lack IFNy. It is plausible that this striking difference may be due to the fact that IFNy^{-/-} T cell
359 chimeric mice had never possessed IFNy-competent T cells, while mice in the CD4+ T cell depletion
360 studies were previously exposed to T cell-derived IFNy, and may have therefore achieved a baseline Th1
361 T cell driven response or tonic state that could support the production of IFNy by other cell types when
362 needed.

363

364 Prior studies showed that IFNy produced by adoptively transferred Th1-polarized, *Mtb* antigen-specific
365 CD4+ T cells is dispensable to control of pulmonary *Mtb* burden in WT host mice(6) when transferred at
366 a dose of 1×10^7 cells/host, and partially dispensable at a dose of 1×10^6 cells/host. Together with our
367 results, these data indicate that high numbers of *Mtb* antigen-specific, Th1-polarized IFNy^{-/-} CD4+ T cells
368 likely amplify the importance of IFNy-independent T cell effects and overcome a requirement for T cell-
369 derived IFNy to reduce *Mtb* burden in the lung, while dependence on T cell-derived IFNy is unmasked at

370 more physiologic numbers of antigen-specific T cells that are more closely aligned with an expected
371 vaccine response.

372
373 One factor that limits the interpretation of our studies is that C57BL/6 mice, the strain used in our work, is
374 known to elicit a Th1-skewed response, whereas other genetic backgrounds may be less dependent on
375 IFN γ for protection against TB (52, 53). Furthermore, Th1-driven mechanisms in C57BL/6 mice may
376 differ from those in humans. While the role of IFN γ -induced NOS2 in *Mtb* restriction is well-established in
377 mice, *Mtb*-infected human peripheral blood-derived monocytes produce only small amounts of nitric
378 oxide in response to IFN γ signaling in vitro(54). Whether NOS2 is induced at sites of *Mtb* infection in
379 human lungs is controversial, with studies showing different results(55–57). Nevertheless, the most
380 frequently cited manuscripts arguing for a minimal role of T cell-derived IFN γ in pulmonary immunity
381 against TB are studies in C57BL/6 mice, which are inconsistent with our results.

382
383 Our study was performed in unvaccinated mice, and it remains possible that vaccination could boost
384 other mechanisms of immunity independently of T cell-derived IFN γ . For example, though prior studies
385 have definitively proven the requirement for IFN γ in control of *Mtb*, IFN γ R $^{-/-}$ mice vaccinated with BCG
386 still have a survival advantage over unvaccinated IFN γ R $^{-/-}$ mice(17); while T cell-independent effects such
387 as trained immunity could be responsible, IFN γ -independent T cell activity may also play a role.
388 Nevertheless, our results indicate that T cell-derived IFN γ can be critical for immunity within the *Mtb*-
389 infected lung and vaccination or host-directed therapy strategies that restore or augment the ability of
390 *Mtb*-specific T cells to produce IFN γ should continue to be explored.

391

392 **ACKNOWLEDGMENTS**

393 We thank Daniel Kim, Lindsay Engels, Kaitlin Durga, and the SCRI Animal Care staff for technical
394 assistance, Alan Diercks for RNA-seq data alignment, SCRI Research Scientific Computing for HPC
395 resources, and other members of the Urdahl Lab for helpful discussions. This study was supported by
396 NIH grants U19AI135976 (K.B.U.), 75N93019C00070 (K.B.U.), and T32AI007044 (K.M.), the Firland
397 Foundation 20230026C (K.M.), the American Lung Association CAALA2023 (K.M.), and the NIH-funded
398 Seattle TB Research Advancement Center (SEATRAC) 1P30AI168034-01 (K.M.). The sponsors had no
399 role in the design, conduct, analysis, or interpretation of the study, nor in the preparation, review, or
400 approval of the manuscript.

401

402 1. Caruso, A. M., N. Serbina, E. Klein, K. Triebold, B. R. Bloom, and J. L. Flynn. 1999. Mice deficient in
403 CD4 T cells have only transiently diminished levels of IFN-gamma, yet succumb to tuberculosis. *J
404 Immunol* 162: 5407–5416.
405 2. Casanova, J.-L., and L. Abel. 2002. Genetic dissection of immunity to mycobacteria: the human
406 model. *Annu Rev Immunol* 20: 581–620.

407 3. Esmail, H., C. Riou, E. du Bruyn, R. P.-J. Lai, Y. X. R. Harley, G. Meintjes, K. A. Wilkinson, and R. J.
408 Wilkinson. 2018. The Immune Response to *Mycobacterium tuberculosis* in HIV-1-Coinfected Persons.
409 *Annu Rev Immunol* 36: 603–638.

410 4. Flynn, J., J. Chan, K. Triebold, D. Dalton, T. Stewart, and B. Bloom. 1993. An essential role for
411 interferon gamma in resistance to *Mycobacterium tuberculosis* infection. *The Journal of experimental*
412 *medicine* 178: 2249–2254.

413 5. Pearl, J. E., B. Saunders, S. Ehlers, I. M. Orme, and A. M. Cooper. 2001. Inflammation and
414 Lymphocyte Activation during Mycobacterial Infection in the Interferon- γ -Deficient Mouse. *Cellular*
415 *Immunology* 211: 43–50.

416 6. Boisson-Dupuis, S., J. Bustamante, J. El-Baghdadi, Y. Camcioglu, N. Parvaneh, S. El Azbaoui, A.
417 Agader, A. Hassani, N. El Hafidi, N. A. Mrani, Z. Jouhadi, F. Ailal, J. Najib, I. Reisli, A. Zamani, S.
418 Yosunkaya, S. Gulle-Girit, A. Yildiran, F. E. Cipe, S. H. Torun, A. Metin, B. Y. Atikan, N. Hatipoglu, C.
419 Aydogmus, S. S. Kilic, F. Dogu, N. Karaca, G. Aksu, N. Kutukculer, M. Keser-Emiroglu, A. Somer, G.
420 Tanir, C. Aytekin, P. Adimi, S. A. Mahdaviani, S. Mamishi, A. Bousfiha, O. Sanal, D. Mansouri, J.-L.
421 Casanova, and L. Abel. 2015. Inherited and acquired immunodeficiencies underlying tuberculosis in
422 childhood. *Immunol Rev* 264: 103–120.

423 7. Majlessi, L., M. Simsova, Z. Jarvis, P. Brodin, M.-J. Rojas, C. Bauche, C. Nouzé, D. Ladant, S. T.
424 Cole, P. Sebo, and C. Leclerc. 2006. An increase in antimycobacterial Th1-cell responses by prime-
425 boost protocols of immunization does not enhance protection against tuberculosis. *Infect Immun* 74:
426 2128–2137.

427 8. Mittrücker, H.-W., U. Steinhoff, A. Köhler, M. Krause, D. Lazar, P. Mex, D. Miekley, and S. H. E.
428 Kaufmann. 2007. Poor correlation between BCG vaccination-induced T cell responses and protection
429 against tuberculosis. *Proc Natl Acad Sci U S A* 104: 12434–12439.

430 9. Jeevan, A., D. L. Bonilla, and M. N David. 2009. Expression of interferon-gamma and tumour necrosis
431 factor-alpha messenger RNA does not correlate with protection in guinea pigs challenged with virulent
432 *Mycobacterium tuberculosis* by the respiratory route. *Immunology* 128: e296–e305.

433 10. Kagina, B. M. N., B. Abel, T. J. Scriba, E. J. Hughes, A. Keyser, A. Soares, H. Gamieldien, M.
434 Sidibana, M. Hatherill, S. Gelderbloem, H. Mahomed, A. Hawkridge, G. Hussey, G. Kaplan, W. A.
435 Hanekom, and other members of the South African Tuberculosis Vaccine Initiative. 2010. Specific T cell
436 frequency and cytokine expression profile do not correlate with protection against tuberculosis after
437 bacillus Calmette–Guérin vaccination of newborns. *Am J Respir Crit Care Med* 182: 1073–1079.

438 11. Abebe, F. 2012. Is interferon-gamma the right marker for bacille Calmette–Guérin-induced immune
439 protection? The missing link in our understanding of tuberculosis immunology. *Clinical and Experimental*
440 *Immunology* 169: 213–219.

441 12. Billeskov, R., J. P. Christensen, C. Aagaard, P. Andersen, and J. Dietrich. 2013. Comparing
442 adjuvanted H28 and modified vaccinia virus ankara expressingH28 in a mouse and a non-human primate
443 tuberculosis model. *PLoS One* 8: e72185.

444 13. Tameris, M., H. Geldenhuys, A. K. Luabeya, E. Smit, J. E. Hughes, S. Vermaak, W. A. Hanekom, M.
445 Hatherill, H. Mahomed, H. McShane, and T. J. Scriba. 2014. The candidate TB vaccine, MVA85A,
446 induces highly durable Th1 responses. *PLoS One* 9: e87340.

447 14. Rodo, M. J., V. Rozot, E. Nemes, O. Dintwe, M. Hatherill, F. Little, and T. J. Scriba. 2019. A
448 comparison of antigen-specific T cell responses induced by six novel tuberculosis vaccine candidates.
449 *PLoS Pathog* 15: e1007643.

450 15. Nandi, B., and S. M. Behar. 2011. Regulation of neutrophils by interferon- γ limits lung inflammation
451 during tuberculosis infection. *Journal of Experimental Medicine* 208: 2251–2262.

452 16. Sakai, S., K. D. Kauffman, M. A. Sallin, A. H. Sharpe, H. A. Young, V. V. Ganusov, and D. L. Barber.
453 2016. CD4 T Cell-Derived IFN- γ Plays a Minimal Role in Control of Pulmonary *Mycobacterium*
454 tuberculosis Infection and Must Be Actively Repressed by PD-1 to Prevent Lethal Disease. *PLOS*
455 *Pathogens* 12: e1005667.

456 17. Cowley, S. C., and K. L. Elkins. 2003. CD4+ T cells mediate IFN-gamma-independent control of
457 *Mycobacterium tuberculosis* infection both in vitro and in vivo. *J Immunol* 171: 4689–4699.

458 18. Gallegos, A. M., J. W. J. van Heijst, M. Samstein, X. Su, E. G. Pamer, and M. S. Glickman. 2011. A
459 Gamma Interferon Independent Mechanism of CD4 T Cell Mediated Control of *M. tuberculosis* Infection
460 in vivo. *PLoS Pathog* 7: e1002052.

461 19. Dis, E. V., D. M. Fox, H. M. Morrison, D. M. Fines, J. P. Babirye, L. H. McCann, S. Rawal, J. S. Cox,
462 and S. A. Stanley. 2022. IFN- γ -independent control of *M. tuberculosis* requires CD4 T cell-derived GM-
463 CSF and activation of HIF-1 α . *PLOS Pathogens* 18: e1010721.

464 20. Scanga, C. A., V. P. Mohan, K. Yu, H. Joseph, K. Tanaka, J. Chan, and J. L. Flynn. 2000. Depletion
465 of CD4(+) T cells causes reactivation of murine persistent tuberculosis despite continued expression of
466 interferon gamma and nitric oxide synthase 2. *J Exp Med* 192: 347–358.

467 21. Surh, C. D., and J. Sprent. 2000. Homeostatic T Cell Proliferation: How Far Can T Cells Be Activated
468 to Self-Ligands? *The Journal of Experimental Medicine* 192: 9.

469 22. Kim, J., J. Y. Lee, K. Cho, S.-W. Hong, K. S. Kim, J. Sprent, S.-H. Im, C. D. Surh, and J.-H. Cho.
470 2018. Spontaneous Proliferation of CD4+ T Cells in RAG-Deficient Hosts Promotes Antigen-Independent
471 but IL-2-Dependent Strong Proliferative Response of Naïve CD8+ T Cells. *Front Immunol* 9: 1907.

472 23. Ancelet, L., F. J. Rich, B. Delahunt, and J. R. Kirman. 2012. Dissecting memory T cell responses to
473 TB: concerns using adoptive transfer into immunodeficient mice. *Tuberculosis (Edinb)* 92: 422–433.

474 24. Falk, I., A. J. Potocnik, T. Barthlott, C. N. Levelt, and K. Eichmann. 1996. Immature T cells in
475 peripheral lymphoid organs of recombinase-activating gene-1/-2-deficient mice. Thymus dependence
476 and responsiveness to anti-CD3 epsilon antibody. *J Immunol* 156: 1362–1368.

477 25. Moguche, A. O., S. Shafiani, C. Clemons, R. P. Larson, C. Dinh, L. E. Higdon, C. J. Cambier, J. R.
478 Sissons, A. M. Gallegos, P. J. Fink, and K. B. Urdahl. 2015. ICOS and Bcl6-dependent pathways
479 maintain a CD4 T cell population with memory-like properties during tuberculosis. *J Exp Med* 212: 715–
480 728.

481 26. Cosma, C. L., O. Humbert, and L. Ramakrishnan. 2004. Superinfecting mycobacteria home to
482 established tuberculous granulomas. *Nat Immunol* 5: 828–835.

483 27. McCarthy, D. J., Y. Chen, and G. K. Smyth. 2012. Differential expression analysis of multifactor RNA-
484 Seq experiments with respect to biological variation. *Nucleic Acids Research* 40: 4288–4297.

485 28. Ji, D. X., L. H. Yamashiro, K. J. Chen, N. Mukaida, I. Kramnik, K. H. Darwin, and R. E. Vance. 2019.
486 Type I interferon-driven susceptibility to *Mycobacterium tuberculosis* is mediated by IL-1Ra. *Nature
487 Microbiology* 4: 2128–2135.

488 29. Moreira-Teixeira, L., K. Mayer-Barber, A. Sher, and A. O'Garra. 2018. Type I interferons in
489 tuberculosis: Foe and occasionally friend. *J Exp Med* 215: 1273–1285.

490 30. Zhang, L., X. Jiang, D. Pfau, Y. Ling, and C. F. Nathan. 2021. Type I interferon signaling mediates
491 *Mycobacterium tuberculosis*-induced macrophage death. *J Exp Med* 218: e20200887.

492 31. Kotov, D. I., O. V. Lee, C. Langner, J. V. Guillen, J. M. Peters, A. Moon, E. M. Burd, K. C. Witt, D. B.
493 Stetson, D. L. Jaye, B. D. Bryson, and R. E. Vance. 2022. Cellular sources and targets of type I
494 interferons that drive susceptibility to tuberculosis. 2022.10.06.511233.

495 32. Berry, M. P., C. M. Graham, M. W Finlay, Z. Xu, S. A. A. Bloch, T. Oni, K. A. Wilkinson, R.
496 Banchereau, J. Skinner, R. J. Wilkinson, C. Quinn, D. Blankenship, R. Dhawan, J. J. Cush, A. Mejias, O.
497 Ramilo, O. M. Kon, V. Pascual, J. Banchereau, D. Chaussabel, and O. Anne. 2010. An interferon-
498 inducible neutrophil-driven blood transcriptional signature in human tuberculosis. *Nature* 466: 973–977.

499 33. Gaffney, E., D. Murphy, A. Walsh, S. Connolly, S. A. Basdeo, J. Keane, and J. J. Phelan. 2022.
500 Defining the role of neutrophils in the lung during infection: Implications for tuberculosis disease. *Front
501 Immunol* 13: 984293.

502 34. Bohrer, A. C., E. Castro, Z. Hu, A. T. L. Queiroz, C. E. Tocheny, M. Assmann, S. Sakai, C. Nelson, P.
503 J. Baker, H. Ma, L. Wang, W. Zilu, E. du Bruyn, C. Riou, K. D. Kauffman, Tuberculosis Imaging Program,
504 I. N. Moore, F. D. Nonno, L. Petrone, D. Goletti, A. R. Martineau, D. M. Lowe, M. R. Cronan, R. J.
505 Wilkinson, C. E. Barry, L. E. Via, D. L. Barber, A. D. Klion, B. B. Andrade, Y. Song, K.-W. Wong, and K.
506 D. Mayer-Barber. 2021. *Eosinophils are an integral component of the pulmonary granulocyte response in
507 Tuberculosis and promote host resistance in mice*,. *Immunology*.

508 35. Buccheri, S., R. Reljic, N. Caccamo, J. Ivanyi, M. Singh, A. Salerno, and F. Dieli. 2007. IL-4 depletion
509 enhances host resistance and passive IgA protection against tuberculosis infection in BALB/c mice. *Eur J
510 Immunol* 37: 729–737.

511 36. Jung, Y.-J., R. LaCourse, L. Ryan, and R. J. North. 2002. Evidence inconsistent with a negative
512 influence of T helper 2 cells on protection afforded by a dominant T helper 1 response against
513 Mycobacterium tuberculosis lung infection in mice. *Infect Immun* 70: 6436–6443.

514 37. Heitmann, L., M. Abad Dar, T. Schreiber, H. Erdmann, J. Behrends, A. N. J. Mckenzie, F.
515 Brombacher, S. Ehlers, and C. Hölscher. 2014. The IL-13/IL-4R α axis is involved in tuberculosis-
516 associated pathology. *J Pathol* 234: 338–350.

517 38. Hölscher, C., L. Heitmann, E. Owusu-Dabo, R. D. Horstmann, C. G. Meyer, S. Ehlers, and T. Thye.
518 2016. A Mutation in IL4RA Is Associated with the Degree of Pathology in Human TB Patients. *Mediators
519 Inflamm* 2016: 4245028.

520 39. Monin, L., K. L. Griffiths, W. Y. Lam, R. Gopal, D. D. Kang, M. Ahmed, A. Rajamanickam, A. Cruz-
521 Lagunas, J. Zúñiga, S. Babu, J. K. Kolls, M. Mitreva, B. A. Rosa, R. Ramos-Payan, T. E. Morrison, P. J.
522 Murray, J. Rangel-Moreno, E. J. Pearce, and S. A. Khader. 2015. Helminth-induced arginase-1
523 exacerbates lung inflammation and disease severity in tuberculosis. *J Clin Invest* 125: 4699–4713.

524 40. Rook, G. A. W. 2007. Th2 cytokines in susceptibility to tuberculosis. *Curr Mol Med* 7: 327–337.

525 41. Sharma, S. K., D. K. Mitra, A. Balamurugan, R. M. Pandey, and N. K. Mehra. 2002. Cytokine
526 polarization in miliary and pleural tuberculosis. *J Clin Immunol* 22: 345–352.

527 42. Mazzarella, G., A. Bianco, F. Perna, D. D'Auria, E. Grella, E. Moscariello, and A. Sanduzzi. 2003. T
528 lymphocyte phenotypic profile in lung segments affected by cavitary and non-cavitary tuberculosis. *Clin
529 Exp Immunol* 132: 283–288.

530 43. van Crevel, R., E. Karyadi, F. Preyers, M. Leenders, B. J. Kullberg, R. H. Nelwan, and J. W. van der
531 Meer. 2000. Increased production of interleukin 4 by CD4+ and CD8+ T cells from patients with
532 tuberculosis is related to the presence of pulmonary cavities. *J Infect Dis* 181: 1194–1197.

533 44. Fenhalls, G., A. Wong, J. Bezuidenhout, P. van Helden, P. Bardin, and P. T. Lukey. 2000. In situ
534 production of gamma interferon, interleukin-4, and tumor necrosis factor alpha mRNA in human lung
535 tuberculous granulomas. *Infect Immun* 68: 2827–2836.

536 45. Lienhardt, C., A. Azzurri, A. Amedei, K. Fielding, J. Sillah, O. Y. Sow, B. Bah, M. Benagiano, A.
537 Diallo, R. Manetti, K. Manneh, P. Gustafson, S. Bennett, M. M. D'Ellos, K. McAdam, and G. Del Prete.
538 2002. Active tuberculosis in Africa is associated with reduced Th1 and increased Th2 activity in vivo. *Eur
539 J Immunol* 32: 1605–1613.

540 46. Aira, N., A.-M. Andersson, S. K. Singh, D. M. McKay, and R. Blomgran. 2017. Species dependent
541 impact of helminth-derived antigens on human macrophages infected with Mycobacterium tuberculosis:
542 Direct effect on the innate anti-mycobacterial response. *PLoS Negl Trop Dis* 11: e0005390.

543 47. Cozmei, C., D. Constantinescu, E. Carasevici, E. Anisie, D. Ungureanu, A. Sorete-Arboare, D.
544 Gramadă, T. Mihăescu, C. Croitoru, and D. Popa. 2007. Th1 and Th2 cytokine response in patients with
545 pulmonary tuberculosis and health care workers occupationally exposed to M. tuberculosis. *Rev Med
546 Chir Soc Med Nat Iasi* 111: 702–709.

547 48. Rook, G. A. W., R. Hernandez-Pando, K. Dheda, and G. Teng Seah. 2004. IL-4 in tuberculosis:
548 implications for vaccine design. *Trends in Immunology* 25: 483–488.

549 49. Das, G., S. Sheridan, and C. A. Janeway. 2001. The source of early IFN-gamma that plays a role in
550 Th1 priming. *J Immunol* 167: 2004–2010.

551 50. Desvignes, L., and J. D. Ernst. 2009. Interferon-gamma-responsive nonhematopoietic cells regulate
552 the immune response to Mycobacterium tuberculosis. *Immunity* 31: 974–985.

553 51. Dalton, D. K., L. Haynes, C. Q. Chu, S. L. Swain, and S. Wittmer. 2000. Interferon gamma eliminates
554 responding CD4 T cells during mycobacterial infection by inducing apoptosis of activated CD4 T cells. *J
555 Exp Med* 192: 117–122.

556 52. Kurtz, S. L., A. P. Rossi, G. L. Beamer, D. M. Gatti, I. Kramnik, and K. L. Elkins. 2020. The Diversity
557 Outbred Mouse Population Is an Improved Animal Model of Vaccination against Tuberculosis That
558 Reflects Heterogeneity of Protection. *mSphere* 5: e00097-20.

559 53. Smith, C. M., R. E. Baker, M. K. Proulx, B. B. Mishra, J. E. Long, S. W. Park, H.-N. Lee, M. C. Kiritsy,
560 M. M. Bellerose, A. J. Olive, K. C. Murphy, K. Papavinasasundaram, F. J. Boehm, C. J. Reames, R. K.
561 Meade, B. K. Hampton, C. L. Linnertz, G. D. Shaw, P. Hock, T. A. Bell, S. Ehrt, D. Schnappinger, F.
562 Pardo-Manuel de Villena, M. T. Ferris, T. R. Ioerger, and C. M. Sassetti. 2022. Host-pathogen genetic
563 interactions underlie tuberculosis susceptibility in genetically diverse mice. *eLife* 11: e74419.

564 54. Jagannath, C., J. K. Actor, and R. L. Hunter. 1998. Induction of nitric oxide in human monocytes and
565 monocyte cell lines by *Mycobacterium tuberculosis*. *Nitric Oxide* 2: 174–186.

566 55. MacMicking, J., Q. W. Xie, and C. Nathan. 1997. Nitric oxide and macrophage function. *Annu. Rev.*
567 *Immunol.* 15: 323–350.

568 56. Choi, H.-S., P. R. Rai, H. W. Chu, C. Cool, and E. D. Chan. 2002. Analysis of nitric oxide synthase
569 and nitrotyrosine expression in human pulmonary tuberculosis. *Am J Respir Crit Care Med* 166: 178–
570 186.

571 57. Mattila, J. T., O. O. Ojo, D. Kepka-Lenhart, S. Marino, J. H. Kim, S. Y. Eum, L. E. Via, C. E. Barry, E.
572 Klein, D. E. Kirschner, S. M. Morris, P. L. Lin, and J. L. Flynn. 2013. Microenvironments in tuberculous
573 granulomas are delineated by distinct populations of macrophage subsets and expression of nitric oxide
574 synthase and arginase isoforms. *J Immunol* 191: 773–784.

575

576 **FIGURE LEGENDS**

577

578 **Figure 1: IFN γ ^{-/-} T cells do not reduce *Mtb* bacterial burden, and exacerbate disease in T cell
579 chimeric mice.**

580 (A) Schematic of the preparation of TCR β ^{-/-}, WT, and IFN γ ^{-/-}, T cell chimeric mice, followed by infection
581 with aerosolized *Mtb*.
582 (B-C) Bacterial burden in lungs and spleens of *Mtb*-infected T cell chimeric mice at 25dpi in one
583 representative experiment (B), as well as group means from six independent experiments (C). Total
584 n=35 TCR β ^{-/-}, n=34 WT, and n=33 IFN γ ^{-/-} T cell chimeric mice. Statistical significance was determined
585 by Tukey's range test. * $p \leq 0.05$, ** $p \leq 0.01$, *** $p \leq 0.001$, **** $p \leq 0.0001$.
586 (D) Weight trends of *Mtb*-infected T cell chimeric mice through 29dpi.

587

588 **Figure 2: Adoptively transferred IFN γ ^{-/-} CD4+ T cells do not reduce *Mtb* burden, and exacerbate
589 disease in TCR β ^{-/-} mice.**

590 (A) Schematic of adoptive transfer of zero (none) or 3*10⁶ WT, 50/50% mixed, or IFN γ ^{-/-} CD4+ T cells to
591 T cell-deficient host mice after infection with aerosolized *Mtb*.
592 (B) Bacterial burden in lungs and spleens of *Mtb*-infected adoptive transfer mice at 36dpi. Results are
593 representative of two independent experiments. Statistical significance was determined by Tukey's range
594 test. * $p \leq 0.05$, ** $p \leq 0.01$, *** $p \leq 0.001$, **** $p \leq 0.0001$.
595 (C) Weight trends of *Mtb*-infected adoptive transfer mice through 36dpi.

596

597 **Figure 3: IFN γ ^{-/-} T cells promote neutrophil and eosinophil recruitment to pulmonary lesions in T
598 cell chimeric mice infected with *Mtb*.**

599 (A) Absolute number of each indicated cell type among live, parenchymal (IV-) cells in the right lung of T
600 cell chimeric mice at 25dpi. Results are representative of six independent experiments. Statistical
601 significance was determined by Tukey's range test. * $p \leq 0.05$, ** $p \leq 0.01$, *** $p \leq 0.001$, **** $p \leq 0.0001$.
602 AM: Alveolar macrophage, MDM: monocyte-derived macrophage, Neut: neutrophil, Eo: eosinophil
603 (B) Representative confocal microscopy demonstrating AMs (SiglecF+, CD68+), MDMs (SiglecF-,
604 CD68+), neutrophils (CD177+), and eosinophils (SiglecF+, CD11c-) in TB lesions in T cell chimeric mice.
605 (C) Representative images of TB lesions in H&E-stained sections of T cell chimeric mice at 25dpi. 40x:
606 arrows represent TB lesions. 200x: asterisks represent perivasculär and peribronchiolar lymphocyte
607 aggregates. 400x: arrows represent neutrophilic infiltrates.
608 (D) Principal component analysis of fifteen histopathologic features assessed in representative sections
609 of fixed and hematoxylin-eosin (H&E) stained lung of T cell chimeric mice at 25dpi. PVLA: perivasculär
610 lymphoid aggregates. PBLA: peribronchial lymphoid aggregates. MNGC: multinucleated giant cells.

611

612 **Figure 4: IFNy^{-/-} T cells drive a Th2 cytokine milieu and alternative activation of monocyte-derived
613 macrophages in T cell chimeric mice infected with *Mtb*.**

614 (A) Relative expression of classical (M1) and alternative (M2) genes in FACS-sorted bystander and *Mtb*-
615 infected MDMs in lungs of T cell chimeric mice at 25dpi.

616 (B) Concentration of Type 2 cytokines in lung lysates from *Mtb*-infected T cell chimeric mice at 25dpi, as
617 measured by cytokine bead array. Results are representative of two independent experiments.

618 (C) Concentration of IFNy in lung lysates from *Mtb*-infected T cell chimeric mice at 25dpi, as measured
619 by Luminex assay. Results are representative of two independent experiments.

620 (D) Representative confocal microscopy demonstrating expression of iNOS and ARG1 in lungs of *Mtb*-
621 infected T cell chimeric mice at 25dpi.

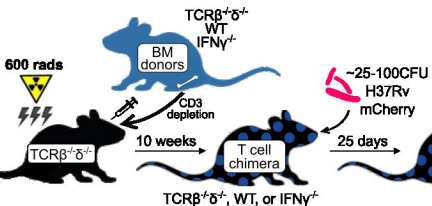
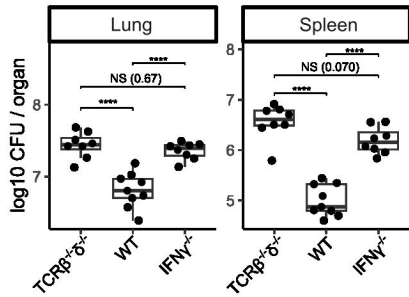
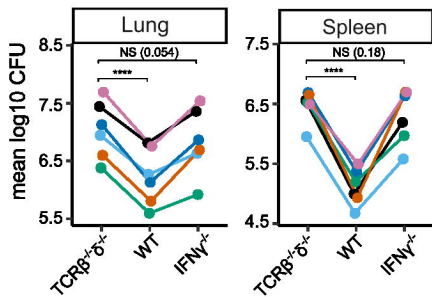
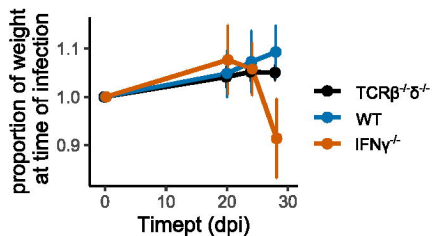
Fig. 1**A****B****C****D**

Fig. 2

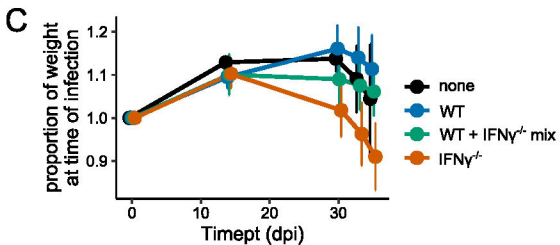
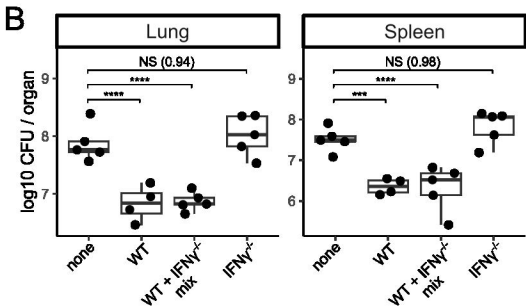
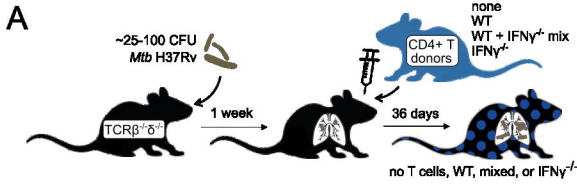
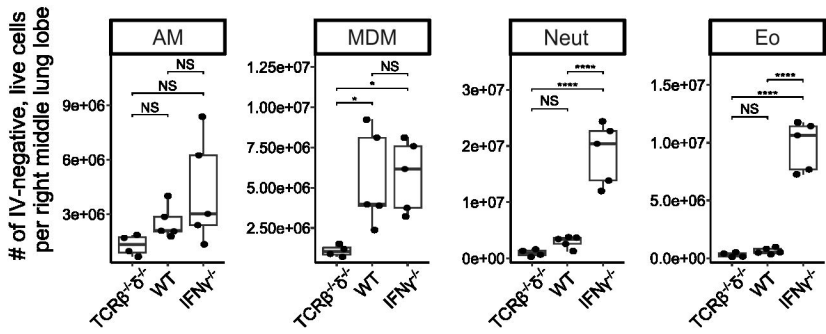
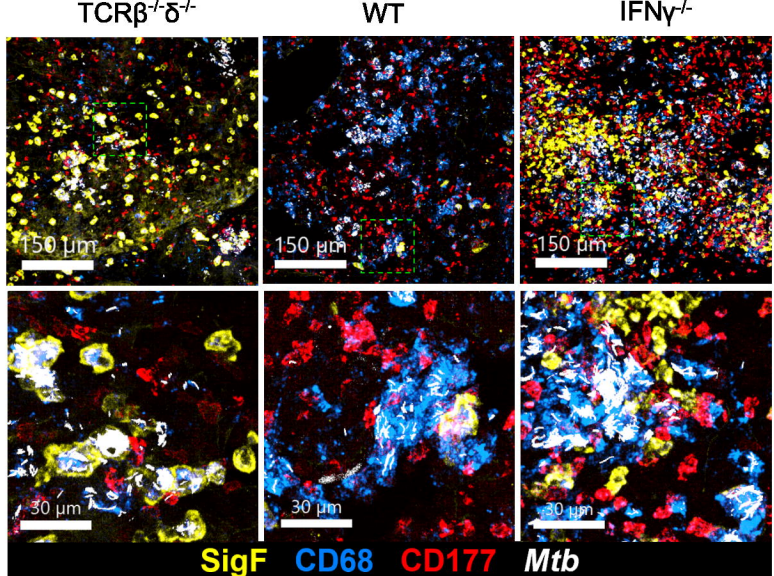


Fig. 3

A



B



C

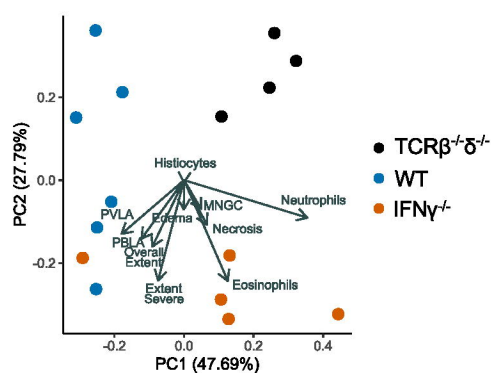
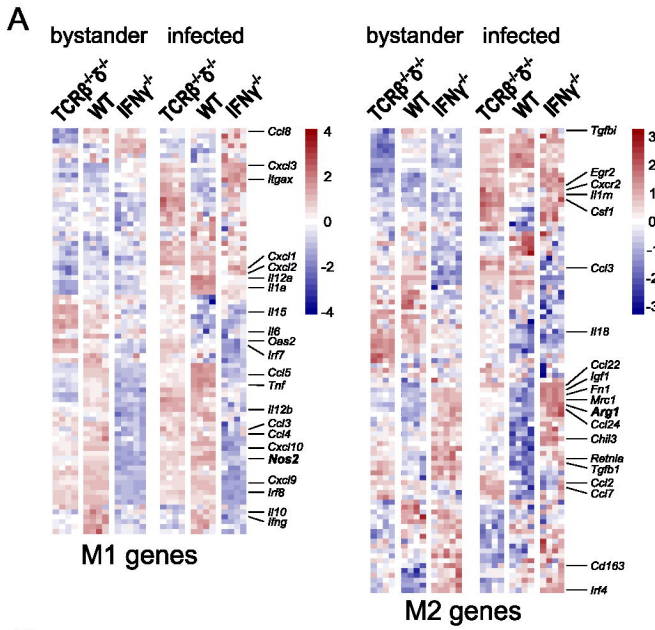


Fig. 4**B**